J Appl Electrochem (2008) 38:1445–1451
DOI 10.1007/s10800-008-9588-1

ORIGINAL PAPER

# Non-platinum electrocatalysts: Manganese oxide nanoparticle-cobaltporphyrin binary catalysts for oxygen reduction

**Mohamed S. El-Deab · Sameh H. Othman · Takeyoshi Okajima · Takeo Ohsaka**

Received: 27 November 2007 / Accepted: 2 May 2008 / Published online: 20 May 2008


**Abstract** This study is concerned with the development of non-platinum electrocatalysts for the efficient 4-electron reduction of molecular oxygen to water in acidic media. A binary catalyst composed of electrodeposited manganese oxide nanoparticles (nano-$MnO_x$) and cobalt porphyrin macro complex (CoP) has been proposed in. The modification of glassy carbon (GC) electrode with CoP alone resulted in a significant positive shift of the oxygen reduction reaction (ORR) compared to the unmodified GC electrode while maintining a 2-electron reduction. That is a positive shift of the onset potential of the ORR of ca. 450 mV was achieved at the former electrode. The modification of the GC electrode with nano-$MnO_x$ alone did not affect the ORR peak potential, but caused a remarkable increase in the reduction peak current due to the catalytic disproportionation of the electrogenerated hydrogen peroxide into water and oxygen. The modification of a GC electrode with CoP and nano-$MnO_x$ (utilizing the advantages of the individual catalysts) resulted in the occurrence of the ORR at a significantly positive potential with almost double peak current compared to the unmodified GC electrode, suggesting a promising procedure for developing electrocatalysts for oxygen reduction in replacement of costly Pt. XPS and SEM techniques were employed to probe the structural and morphological characterization of the proposed binary catalysts.

**Keywords** Oxygen reduction · Macrocyclic compounds · Manganese oxide · Binary catalysts · Hydrogen peroxide

M. S. El-Deab · S. H. Othman · T. Okajima · T. Ohsaka (✉)
Department of Electronic Chemistry, Tokyo Institute of Technology, 4259 Nagatsuta, Midori-ku, Yokohama 226-8502, Japan
e-mail: ohsaka@echem.titech.ac.jp

M. S. El-Deab
Department of Chemistry, Faculty of Science, Cairo University, Cairo, Egypt

*Present Address*:
M. S. El-Deab
Institute of Electrochemistry, Ulm University, 89069 Ulm, Germany
e-mail: msaada68@yahoo.com

S. H. Othman
Second Research Reactor, Nuclear Research Center, Atomic Energy Authority, Cairo 13759, Egypt

## 1 Introduction

The electrocatalytic reduction of molecular oxygen ($O_2$) to water ($H_2O$) at a reasonably low overpotential through a 4-electron reduction pathway has been the aim of numerous investigations. This reaction plays a vital role in electrochemical energy conversion systems such as fuel cells. Many sorts of electrocatalyst for oxygen reduction have been investigated either in alkaline or acidic media. The superiority of Pt as an electrocatalyst for the ORR in acidic media is indisputable; however, special emphasis is being paid to the development of non-platinum electrocatalysts in view of the high cost of Pt and the expected rapid depletion of its natural sources. The development of efficient non-platinum electrocatalysts for the oxygen reduction reaction (ORR) is the ultimate goal of much research [1–20]. In this regard, metallophthalocyanines, metalloporphyrins and related macrocyclic complexes have been investigated [21, 22]. These macrocyclic complexes can be employed to modify the surface of a relatively inert substrate (e.g., glassy carbon (GC)) and thus lead to an enhancement in the adsorption of oxygen molecules at the electrode surface

[23–25]. A significant positive shift of the ORR peak potential may be observed, but the reaction is only limited to a 2-electron reduction pathway. On the other hand, manganese oxides ($MnO_x$), including $MnO_2$, $Mn_2O_3$, $Mn_3O_4$, $Mn_5O_8$ and MnOOH, having economic and environmental advantages, have been used for a long time in air electrodes as electrocatalysts for the reduction of $O_2$, in addition to their wide use as highly active and thermally stable catalysts in industrial and environmental applications [24–36]. These oxides, especially MnOOH, have a good catalytic disproportionation activity towards the decomposition of hydrogen peroxide into water and molecular oxygen [37–39]. In the current study, the combined use of electrochemically deposited manganese oxide nanorods along with some macro cyclic porphyrin complexes has been suggested as a promising procedure for developing efficient non-Pt electrocatalysts for the ORR at a reasonably low cathodic overpotential while supporting an apparent 4-electron reduction pathway of molecular oxygen in acidic media. Three different porphyrins were used, namely, 5, 10, 15, 20-tetrakis(4-methoxyphenyl)-21H,23H-porphine cobalt(II), 5, 10, 15, 20-tetraphenyl-21H,23H-porphine cobalt (II) and 5, 10, 15, 20-tetraphenylporphyrinatoiron(III) chloride, in addition to 2, 3, 9, 10, 16, 17, 23, 24-octacyanophthalocyaninocobalt(II). These macro cyclic metal complexes were selected in view of their significant electrocatalytic effect on the ORR in terms of the positive shift of its onset potential. However, the ORR is still limited to a 2-electron reduction pathway. Thus, the electrodeposition of nano-$MnO_x$ is carried out with the expectation of a conversion of the 2-electron ORR into an effective 4-electron ORR via the catalytic decomposition of hydrogen peroxide into water at the nano-$MnO_x$.

## 2 Experimental

### 2.1 Electrodes

A glassy carbon (GC) electrode (3 mm in diameter) was used as the working electrode. Pt wire and Ag/AgCl/KCl(sat) electrodes were used as the counter and reference electrodes, respectively. The GC electrode was mechanically polished first with no. 2000 emery paper and then with aqueous slurries of successively finer alumina powder (particle size down to 0.06 μm) on a polishing microcloth. The polished electrode was then sonicated in water for 15 min after each polishing step and then rinsed with de-ionized Milli-Q Millipore water.

### 2.2 Preparation of manganese oxide nanoparticles–porphyrin complex modified GC electrode

The thus-polished GC electrodes were electrolyzed in aqueous solution containing 0.1 M $Na_2SO_4$ in the presence/absence of 0.01 M $Mn(CH_3COO)_2$ via cycling the potential between 0 and 1.7 V versus Ag/AgCl/KCl(sat) at a scan rate of 20 mV $s^{-1}$ for 10 potential cycles to electrodeposit $MnO_x$ nanoparticles (nano-$MnO_x$). In the absence of $Mn(CH_3COO)_2$, the bare GC is electro-oxidized (Eox-GC). This was done to improve the adhesion properties of the electrodeposited nano-$MnO_x$ and/or the porphyrin modifiers onto the GC substrate. The Eox-GC and the nano-$MnO_x$ modified GC electrodes were subsequently immersed in 0.05 mM 5, 10, 15, 20-tetrakis(4-methoxyphenyl)-21H, 23H-porphine cobalt(II), 5, 10, 15, 20-tetraphenyl-21H, 23H-porphine cobalt (II), 5, 10, 15, 20-tetraphenylporphyrinatoiron(III) chloride and 2, 3, 9, 10, 16, 17, 23, 24-octacyanophthalocyaninocobalt(II), referred to hereafter as MPPCo, PPCo, PPFe and OCPCo, respectively, (dissolved in DMF) for 30 s to allow for the attachment of the prophyrin molecules to the electrode surface.

### 2.3 Characterizations of the modified GC electrodes

For the morphological characterization of the modified GC electrodes, SEM images of the electrode surface were obtained using a JSM-T220 scanning electron microscope (JEOL, Japan) at an acceleration voltage of 15 kV and a working distance of 4-5 mm Subsequently, the modified GC electrodes were subjected to EDX analysis to identify the elemental species co-existing on the GC surface.

The XPS data were acquired with GC electrodes (6 mm in diameter), which were prepared as mentioned above. The XPS spectra were recorded by an ESCA-3400 electron spectrometer (SHIMADZU) using an unmonochromatized X-ray source with Mg K alpha (1253.6 eV) anode.

### 2.4 Catalytic activity of the modified GC electrodes towards the ORR

Cyclic and steady-state voltammetric measurements were carried out to characterize the catalytic activity of the modified GC electrodes with various modifications towards oxygen reduction in acidic media ($O_2$-saturated 0.1 M $H_2SO_4$), i.e., before and after soaking in 0.05 mM of the respective metalloporphyrins derivative for 30 s. All the electrochemical experiments were carried out in a conventional two-compartment three-electrode Pyrex glass cell using a computer-controlled BAS 100 B/W electrochemical analyzer. Steady-state voltammograms were obtained at a GC disk (3.0 mm)–Pt ring rotating ring disk electrode using a Nikko Keisoku system (Japan) coupled with an ALS/chi 832A electrochemical analyzer bipotentiostat (USA). The working electrode compartment was 200 $cm^3$ to eliminate any possible change of the $O_2$ concentration during the measurements. Prior to each experiment, $O_2$ gas was bubbled directly into the cell for 30 min to obtain an

$O_2$-saturated 0.1 M $H_2SO_4$ solution; during every measurement $O_2$ gas was flushed over the cell solution and the potential scan rate was 0.1 V $s^{-1}$.

## 3 Results and discussion

### 3.1 Characterizations and morphology

Figure 1a–e shows typical SEM micrographs of the Eox-GC electrodes modified with nano-$MnO_x$ electrodeposited from 0.1 M $Na_2SO_4$ containing 0.01 M $Mn(CH_3COO)_2$ aqueous solution by applying (a–c) 5, (d) 25 and (e) 10 potential cycles between 0 and 1.7 V versus Ag/AgCl/KCl(sat) at a scan rate of 20 mV $s^{-1}$. In cases b and c, after electrodeposition of nano-$MnO_x$ the electrodes were further soaked in DMF solution of 0.05 mM MPPCo for (b) 30 and (c) 180 s. This figure shows that the nano-$MnO_x$ is electrodeposited in a porous texture composed of intersected threads (i.e., reticulated vitreous carbon (RVC)-like morphology). This texture covers the entire surface of the electrode homogeneously in a rather porous morphology, which enables access of the solution species to the underlying GC substrate.

The modified GC electrodes (shown in Fig. 1) were subsequently subjected to EDX analysis to identify the elemental species co-existing at the GC surface. Table 1 shows the relative weight percentage (wt%) of the four elements C, Mn, O and Co of the corresponding images shown in Fig. 1. Inspection of this table reveals the following points:

(i) The wt% of Mn increases with increasing cycle number employed during the electrodeposition of the nano-$MnO_x$ concurrently with a decrease in the wt% of C of the underlying substrate. This points to a decrease of the porosity of the nano-$MnO_x$ film atop the GC electrode (compare samples a, d and e).
(ii) The soaking of the nano-$MnO_x$ modified GC electrodes in the MPPCo solution resulted in its effective attachment to the electrode surface, as evident from the detectable amounts of Co (see samples b and c).

Further characterization was carried out to identify the elements that coexist at the modified GC surface and to probe their oxidation state by XPS. The results are shown in Fig. 2A–C, in which the spectra of (A) C 1s, (B) Mn 2p and (C) O 1s are obtained at (a) Eox-GC, (b) MPPCo modified Eox-GC, (c) nano-$MnO_x$ modified Eox-GC and (d) MPPCo and nano-$MnO_x$ modified Eox-GC electrodes. Inspection of this figure reveals the following points: (i) Fig. 2A (curves a–d) shows that there is no significant change in the binding energies of the C 1s upon loading of either the nano-$MnO_x$ or the MPPCo. This indicates that the electronic structure of the GC surface remains effectively the same before and after loading of the nano-$MnO_x$. Thus, the enhancement of the electrocatalytic performance by the nano-$MnO_x$ loading (cf. Fig. 3) does not originate from a change in the electronic properties of the GC surface atoms. (ii) Fig. 2B indicates that Mn exists in a cationic state rather than in an elemental state as evidenced from the positive shift of the 2p binding energy of Mn (i.e., a shift from 650 and 638.8 eV for $2p_{1/2}$ and $2p_{3/2}$, respectively, of elemental Mn, to 653.8 and 641.7 eV in the samples). And (iii) the XPS spectrum of the oxygen in the $MnO_x$ (Fig. 2C) shows a single and rather broad peak for the Eox-GC (Fig. 2C, curve a) corresponding to the C–O bond formed during the electro-oxidative pretreatment of the GC substrate. This peak is developed into a peak with a shoulder upon electrodeposition of the nano-$MnO_x$ (Fig. 2C, curves c and d). The origin of this split may be attributed to the existence of oxygen in hydroxide and oxide forms in MnOOH [40].

### 3.2 Electrocatalytic activity of the nano-$MnO_x$-porphyrin modified GC electrodes towards the ORR

#### *3.2.1 Modification of GC electrode with different porphyrin complexes*

Figure 3 shows typical cyclic voltammograms (CVs) for the ORR at (a) bare Eox-GC, (b) MPPCo, (c) PPCo, (d) PPFe and (e) OCPCo-modified GC electrodes in $O_2$-saturated 0.1 M $H_2SO_4$. The different macrocyclic complexes were confined at the GC electrodes by soaking in a DMF solution of 0.05 mM of the respective macro cyclic metal complex for 30 s. Fig. 4 shows are the corresponding cyclic voltammetric blank responses obtained in $N_2$-saturated 0.1 M $H_2SO_4$ at 100 mV $s^{-1}$. Figure 3 shows that:

(i) Modification of the GC electrodes with any of the four above-mentioned macrocyclic metal complexes resulted in a significant positive shift of the ORR peak potential (from about −0.5 V at the unmodified Eox-GC (curve a)) to different extents. The highest positive shift was obtained at the MPPCo (curve b), that is a 450 mV positive shift of the onset potential compared to the unmodified GC electrode.
(ii) The ORR proceeds, mainly, via a 2-electron reduction pathway at the modified GC electrodes (curves b, d and e) similarly to that obtained at the unmodified GC electrode (curve a) as evident from the almost identical peak current at these electrodes. At the PPFe-modified electrode (curve c), the ORR peak current is almost twice that observed at the unmodified GC (curve a). This observation may be attributed

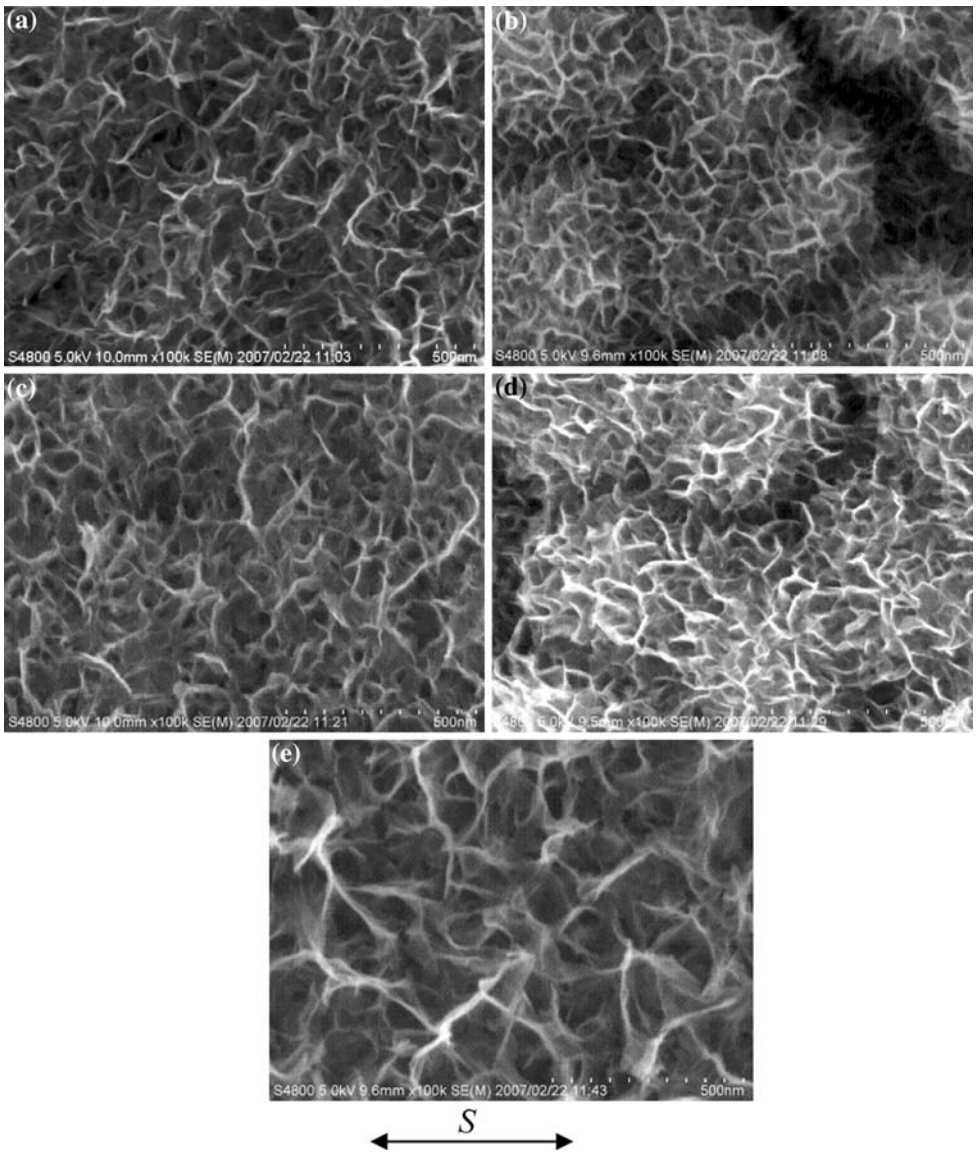


**Fig. 1** SEM images of GC electrodes modified with nano-$MnO_x$ electrodeposited from an aqueous solution of 0.1 M $Na_2SO_4$ containing 0.01 M $Mn(CH_3COO)_2$ by applying (**a**–**c**) 5, (**d**) 25, and (**e**) 10 cycles between 0 and 1.7 V versus Ag/AgCl/KCl(sat). In cases **b** and **c**, nano-$MnO_x$ modified GC electrodes were further soaked in 0.05 mM MPPCo for (**b**) 30 and (**c**) 180 s. $S = 500$ nm,

**Table 1** Variation of the weight percentage of C, O, Mn and Co at the surface of the modified Eox-GC subjected to different modification steps. The same notations of the electrodes as in Fig. 1 are used here

| Sample # | C (%) | Mn (%) | O (%) | Co (%) |
|---|---|---|---|---|
| a | 37.23 | 16.04 | 46.73 | – |
| b | 40.97 | 14.28 | 44.69 | 0.06 |
| c | 61.72 | 6.02 | 32.16 | 0.10 |
| d | 3.53 | 53.01 | 43.46 | – |
| e | 9.09 | 42.24 | 48.68 | – |

to the reduction of molecular oxygen to water, via a 4-electron reduction pathway at this modified electrode [41]. However, a major disadvantage of this electrode (curve c) is the relatively negative peak potential compared to the MPPCo-modified GC electrode (curve b). Thus, MPPCo seems to be a suitable candidate. Hence, further modification of the MPPCo-modified GC electrode with the electrodeposition of manganese oxide was carried out with a view to effecting the 4-electron reduction pathway via the catalytic disproportionation of the electrogenerated hydrogen peroxide by the nano-$MnO_x$ [37–39].

Figure 4 shows no clear redox response for the porphyrin moieties (curves a–d), and only a redox peak couple can be observed in the potential region of 250 to 350 mV arising from the quinone/hydroquinone (Q/HQ) redox couple of the oxidized GC substrate. It is likely presumed here that the redox response of the different porphyrins is either very small compared to the high charging background current of the GC substrate or overlapped with the Q/HQ redox peak potential. Curve e shows a clear redox response of the phthalocyanine ring at ca. −300 mV.

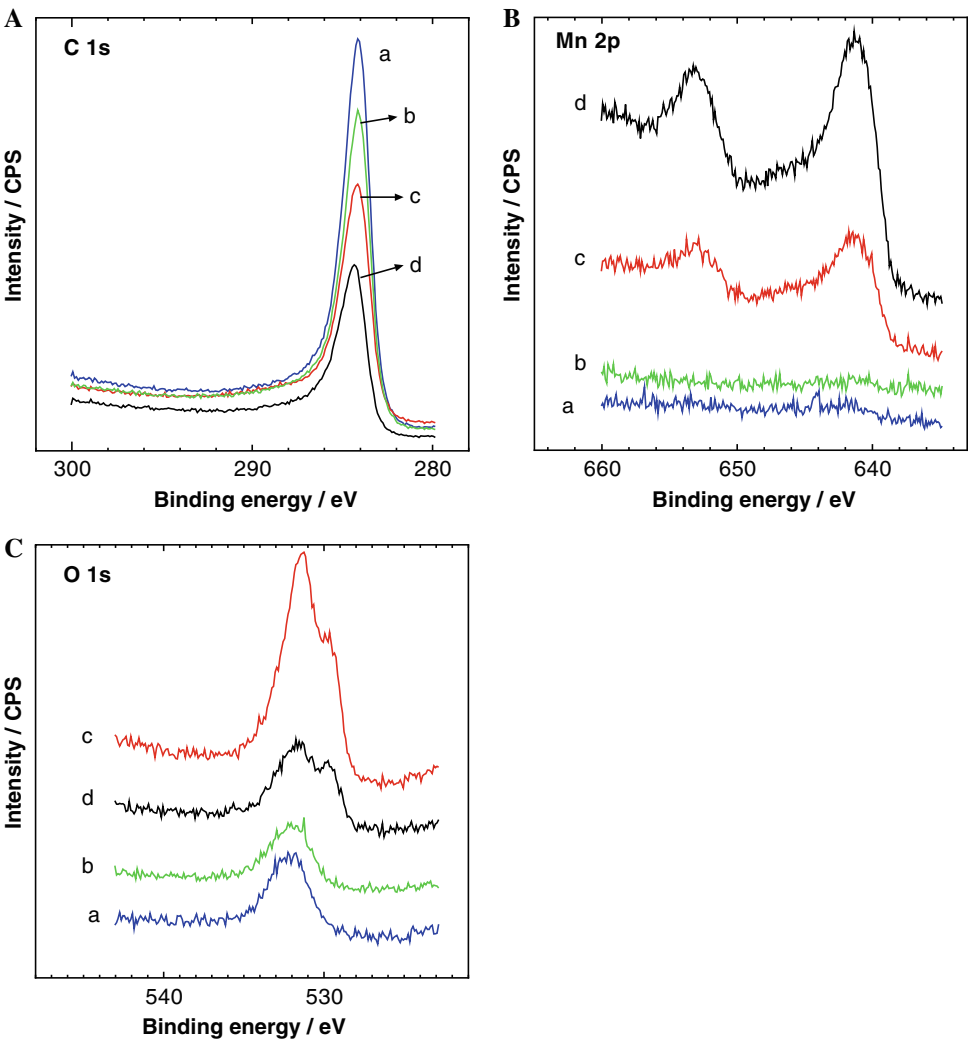


**Fig. 2** XPS spectra of (A) C 1s, (B) Mn 2p and (C) O 1s obtained for (**a**) Eox-GC, (**b**) MPPCo-modified Eox-GC, (**c**) nano-$MnO_x$ modified Eox-GC and (**d**) MPPCo and nano-$MnO_x$ modified Eox-GC electrodes

### 3.2.2 *Modification of GC electrode with nano-$MnO_x$ together with porphyrin complex*

Nano-$MnO_x$ was electrodeposited onto the GC electrode prior to modification with MPPCo, with the expectation of effecting an overall 4-electron reduction of $O_2$. Fig. 5 shows the CVs obtained at (a) bare Eox-GC and Eox-GC electrodes modified with (b) nano-$MnO_x$, (c) MPPCo and (d) nano-$MnO_x$ and MPPCo, measured in $O_2$-saturated 0.1 M $H_2SO_4$ at 100 mV $s^{-1}$. The ORR takes place at the same potential at both the nano-$MnO_x$ modified GC (curve b) and the unmodified GC (curve a) electrodes with a noticeable increase in reduction peak current at the former electrode. This suggests an effective disproportionation of the electrogenerated hydrogen peroxide by the electrodeposited nano-$MnO_x$. That is, the ORR proceeds via a 2-electron reduction reaction at the bare spots of the Eox-GC substrate, which is subsequently followed by a catalytic decomposition of the produced hydrogen peroxide (into water and molecular oxygen) at the nearby nano-$MnO_x$ according to:

$$O_2 + 2H^+ + 2e^- \xrightarrow{C-substrate} H_2O_2 \quad (1)$$

and,

$$H_2O_2 \xrightarrow{nano-MnO_x} 1/2O_2 + H_2O \quad (2)$$

On the other hand, at the MPPCo-modified GC electrode, a significant positive shift of the ORR peak potential was achieved with almost the same peak current as that at the unmodified GC electrode (curve c). Interestingly, a noticeable increase in the peak current was observed upon further modification of the MPPCo-modified GC electrode with nano-$MnO_x$ (curve d). That is, the positive shift is obtained as a result of the catalytic role of the Co porphyrin complex towards the 2-electron reduction of oxygen to hydrogen peroxide ($H_2O_2$). The increase in the peak current is attributable to the catalytic decomposition of the

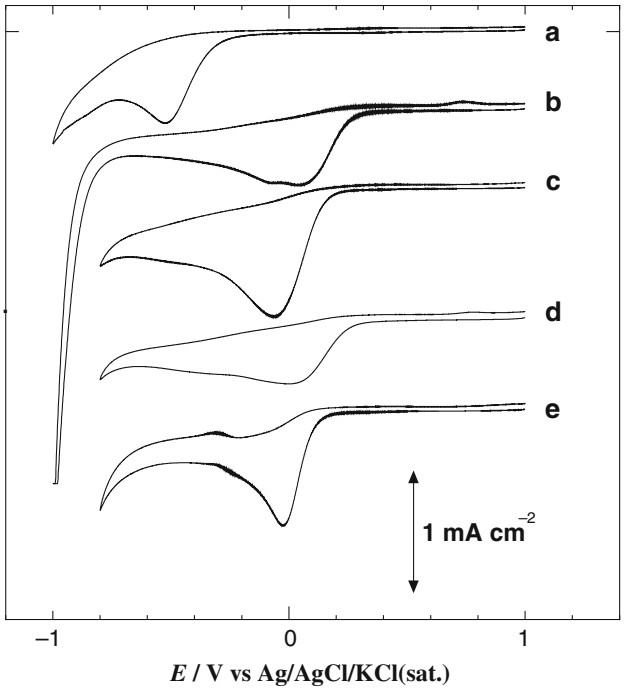


**Fig. 3** CVs for the ORR measured in $O_2$-saturated 0.1 M $H_2SO_4$ at (**a**) bare Eox-GC electrode and (**b**) MPPCo, (**c**) PPCo, (**d**) PPFe and (**e**) OCPCo-modified GC electrodes. Potential scan rate: 100 mV/s

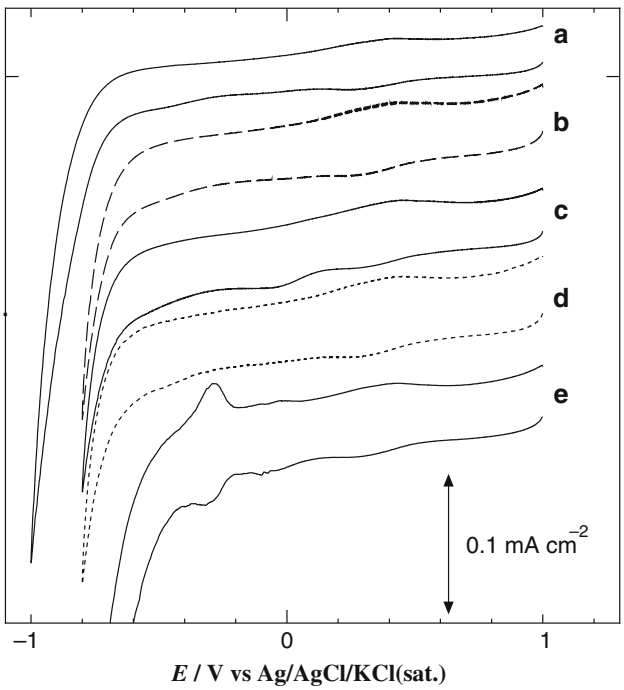


**Fig. 4** Blank CVs response measured in $N_2$-saturated 0.1 M $H_2SO_4$ at the same electrodes as used in Fig. 3. Potential scan rate: 100 mV/s

electrogenerated $H_2O_2$ (to water and molecular oxygen) at the nano-$MnO_x$. Thus, an apparent 4-electron reduction pathway of $O_2$ would be verified at the proposed binary catalysts system.

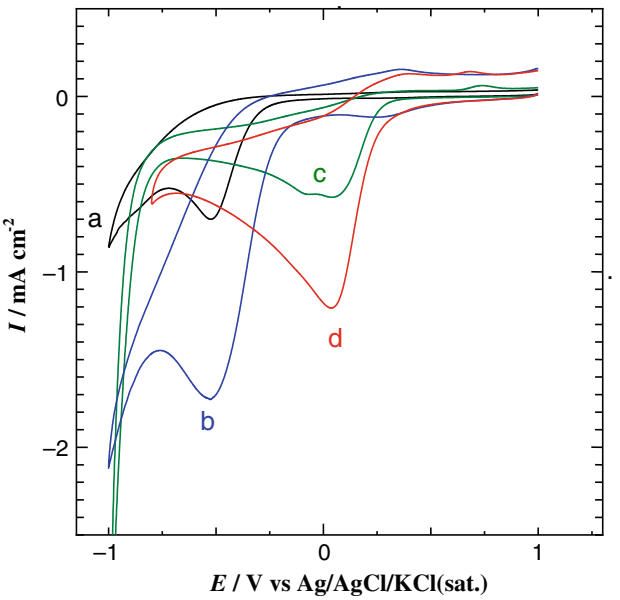


**Fig. 5** CVs obtained at (**a**) bare GC and GC electrodes modified with (**b**) nano-$MnO_x$, (**c**) MPPCo, and (**d**) MPPCo and nano-$MnO_x$, measured in $O_2$-saturated 0.1 M $H_2SO_4$. Potential scan rate: 100 mV/s

### *3.2.3 Steady-state hydrodynamic voltammetry*

Figure 6 shows the steady-state hydrodynamic voltammograms of the ORR at the rotating ring disk electrodes in which the GC disk electrodes are (a) bare Eox-GC and Eox-GC electrodes modified with (b) nano-$MnO_x$, (c) MPPCo and (d) nano-$MnO_x$ and MPPCo, measured in $O_2$-saturated 0.1 M $H_2SO_4$ at a scan rate of 10 mV $s^{-1}$. The ring electrode was a bare Pt electrode (potentiostated at 1.1 V). The lower set of curves (a–d) refers to the ORR at the GC disk electrodes subjected to different modifications, whereas the upper set (a′–d′) refers to the simultaneously measured Pt ring current, which is used as a probe to monitor the amount of electrogenerated hydrogen peroxide at the relevant disk electrode. The positive shift of the onset potential of the ORR is significantly observed at the MPPCo-modified GC electrode in comparison with the unmodified electrode (compare curves a and c). Also the increase in disk current at the nano-$MnO_x$ modified GC disk electrode (curve b) suggests a significant contribution of the 4-electron reduction pathway of $O_2$ at this electrode. Furthermore, modification of the GC disk electrode with MPPCo together with nano-$MnO_x$ resulted in a significant increase in disk current (curve d) with a concurrent decrease in the corresponding ring current (curve d′). This finding points to the contribution of the 4-electron reduction pathway of molecular oxygen becoming more significant at the proposed binary catalyst system at a fairly positive potential.

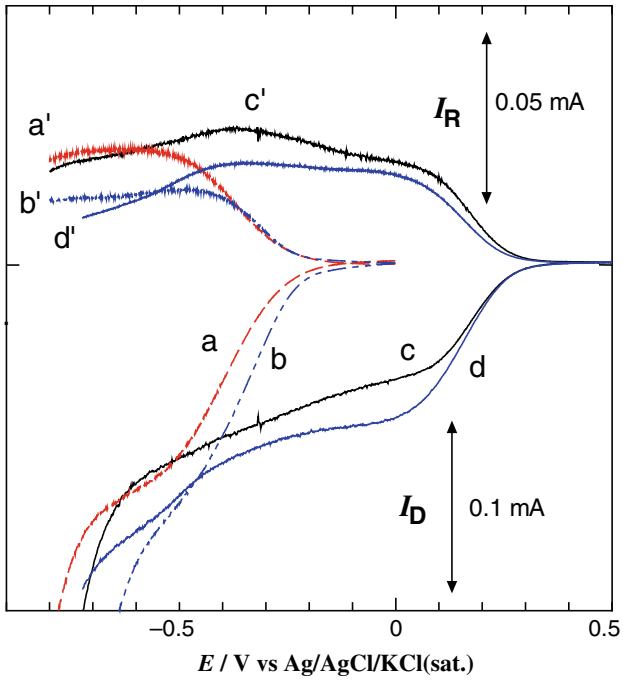


**Fig. 6** Steady-state voltammograms for the ORR obtained at (**a**) bare GC and GC electrodes modified with (**b**) nano-$MnO_x$, (**c**) MPPCo, and (**d**) MPPCo and nano-$MnO_x$, measured in $O_2$-saturated 0.1 M $H_2SO_4$. Rotation rate: 800 rpm. Potential scan rate: 10 mV $s^{-1}$. The corresponding Pt ring currents (potentiostated at 1.1 V) are shown as curves a′–d′

## 4 Conclusion

This paper describes the fabrication of non-platinum electrocatalysts as cathodes for the oxygen reduction reaction in acidic media. The modification of glassy carbon electrodes with electrodeposited manganese oxide nanorods along with porphyrin complex resulted in the achievement of the ORR at a fairly positive potential, that is 450 mV more positive than that obtained at the unmodified GC electrode in $O_2$-saturated 0.1 M $H_2SO_4$ aqueous solution, concurrently with a significant contribution of 4-electron reduction of molecular oxygen.

**Acknowledgements** This work was financially supported by Grant-in-Aid for Scientific Research (A) (No. 19206079) from the Ministry of Education, Culture, Sports, Science and Technology (MEXT), Japan and also by New Energy and Industrial Technology Development Organization (NEDO), Japan. M. S. El-Deab thanks the Japan Society for the Promotion of Science (JSPS) for the Invitation fellowship.

## References

1. Ohsaka T, El-Deab MS (2004) Development of non-platinum-based electrocatalysts for oxygen reduction. In: Recent research developments in electrochemistry, vol 7. Transworld Research Network Publisher, India
2. Kinoshita K (1992) Electrochemical oxygen technology, Wiley
3. Markovic NM, Ross PN (2002) Surf Sci Rep 45:117 (And the references cited therein)
4. Brian CH, Heinzel A (2001) Nature 414:345
5. Watanabe M, Igarashi H, Yoshioka K (1995) Electrochim Acta 40:329
6. Anderson AB, Roques J, Mukerjee S, Murthi VS, Markovic NM, Stamenkovic V (2005) J Phys Chem B 109:1198 (And the references cited therein)
7. Schmidt TJ, Paulus UA, Gasteiger HA, Behm RJ (2001) J Electroanal Chem 508:41
8. Markovic NM, Adzic RR, Cahan BD, Yeager E (1994) J Electroanal Chem 377:249
9. Paffet MT, Beery JG, Gottesfeld S (1988) J Electrochem Soc 135:1431
10. Hu F-PX, Zhang -G, Xiao F, Zhang J-L (2005) Carbon 43:2931
11. Bergel A, Feron D, Mollica A (2005) Electrochem Commun 7:900
12. Singh RN, Lal B, Malviya M (2004) Electrochim Acta 49:4605
13. Dafydd H, Worsley DA, McMurray HN (2005) Corros Sci 47b:3006
14. Feria OS, Duron S (2002) Int J Hydrogen Energy 27:451
15. Lin Y, Cui X, Ye X (2005) Electrochem Commun 7:267
16. Born M, Bogdanoff P, Fiechter S, Tributsch H (2005) J Electroanal Chem 578:339
17. Hernandez J, Gullon JS, Herrero E (2004) J Electroanal Chem 574:185
18. Leger J-M (2005) Electrochim Acta 50:3123
19. Zhang D, Chi D, Okajima T, Ohsaka T (2007) Electrochim Acta 52:5400
20. Arihara K, Mao L, Liddell PA, Ochoa EM, Moore AL, Imase T, Zhang D, Sotomura T, Ohsakaa T (2004) J Electrochem Soc 151:A2047
21. Gojkovic S Lj, Gupta S, Savinell RF (1999) Electrochim Acta 45:889–897
22. Mao L, Arihara K, Sotomura T, Ohsaka T (2004) Electrochim Acta 49:2515–2521
23. Chen J, Zhang W, Officer D, Swiegers GF, Wallace GG (2007) Chem Comm 32
24. Popovici S (1999) J Porph Phthaloc 3:4
25. Shentu B, Oyaizu K, Nishide H (2002) Chem Lett 7
26. El-Deab MS, Awad MI, Mohammad AM, Ohsaka T (2007) Electrochem Commun 9:2082
27. Brock SL, Duan N, Tian ZR, Giraldo O, Zhou H, Suib SL (1998) Chem Mater 10:2619
28. Chen J, Jin JC, Purohit V, Cutlip MB, Suib SL (1997) Catal Today 33:205
29. Hoare JP (1968) The electrochemistry of oxygen, Wiley
30. Yano T, Tryk DA, Hashimoto K, Fujishima A (1998) J Electrochem Soc 145:1870
31. Morcos I, Yeager E (1970) Electrochim Acta 15:953
32. Taylor RJ, Humffray AA (1975) J Electroanal Chem 54:63
33. Matsumoto F, Uesugi S, Koura N, Okajima T, Ohsaka T (2001) J Electroanal Chem 505:150
34. Yano T, Popa E, Tryk DA, Hashimoto K, Fujishima A (1999) J Electrochem Soc 146:1081
35. Hossain MS, Tryk DA, Yeager E (1989) Electrochim Acta 34:1733
36. Wiesener K (1986) Electrochim Acta 31:1073
37. Mao L, Zhang D, Sotomura T, Nakatsu K, Koshiba N, Ohsaka T (2003) Electrochim Acta 48:1015
38. Mao L, Sotomura T, Nakatsu K, Koshiba N, Zhang D, Ohsaka T (2002) J Electrochem Soc 149:A504
39. Ohsaka T, Mao L, Arihara K, Sotomura T (2004) Electrochem Commun 6:273
40. El-Deab MS, Ohsaka T (2006) Angew Chem Int Ed 45:5963
41. Gojkovic SL, Gupta S, Savinell RF (1999) Electrochim Acta 45:889